

Beam polarization effects on top-pair production at the ILC

Nhi M. U. Quach^{a,b*}, Yoshimasa Kurihara^b, Khiem H. Phan^c, Takahiro Ueda^d

^a *The Graduate University for Advanced Studies (SOKENDAI), Hayama, Kanagawa 240-0193, Japan.*

^b *High Energy Accelerator Research Organization (KEK), Tsukuba, Ibaraki 305-0801, Japan.*

^c *University of Science Ho Chi Minh City, 227 Nguyen Van Cu, Dist.5, Ho Chi Minh City, Vietnam.*

^d *Nikhef, Science Park 105 1098 XG Amsterdam, Netherlands.*

Abstract

Full one-loop electroweak-corrections for an $e^-e^+ \rightarrow t\bar{t}$ process associated with sequential $t \rightarrow b\mu\nu_\mu$ decay are discussed. At the one-loop level, the spin-polarization effects of the initial electron and positron beams are included in the total and differential cross sections. A narrow-width approximation is used to treat the top-quark production and decay while including full spin correlations between them. We observed that the radiative corrections due to the weak interaction have a large polarization dependence on both the total and differential cross sections. Therefore, experimental observables that depend on angular distributions such as the forward-backward asymmetry of the top production angle must be treated carefully including radiative corrections. We also observed that the energy distribution of bottom quarks is majorly affected by the radiative corrections.

Keywords: ILC experiment, top-pair production, electroweak radiative correction, beam polarization.

1. Introduction

The discovery of the Higgs boson[1, 2] in 2012 showed the standard theory of particle physics to be well established. Even though the standard theory can describe the microscopic nature at a subatomic level very precisely[3], it cannot be the most fundamental theory of nature because, for instance, it includes many parameters (e.g., particle masses and couplings, number of generations) that are not determined within the theory. While experiments at the Large Hadron Collider continue to search for signals beyond the standard model (BSM), none have been reported to date¹. Besides discovering new particles, pursuing the BSM also involves precise measurements of the properties of known particles. Milestones along this direction must surely be the Higgs boson and the top quark. Because the top quark is the heaviest fermion with a mass above even the electroweak symmetry-breaking scale, it is naturally expected to play a special role in the BSM. In addition, it has been pointed out that the vacuum stability of the Higgs potential depends strongly on the Higgs and top-quark masses[6]. Hence, the precise measurement

¹For the most up-to-date results, see [4] for ATLAS and [5] for CMS collaborations.

of top-quark properties is crucial for understanding the stability of the universe, as well as in the search for BSM signals.

The International Linear Collider(ILC)[7], which is a proposed electron positron colliding experiment with centre-of-mass (CM) energies above 250 GeV, is being discussed intensively as a future project in high-energy physics. The main goals of ILC experiments would be a precise measurement of the Higgs and top-quark properties as well as searching directly for new particles. The ILC will use spin-polarized beams for both its electron and positron beams[8, 9] to increase its sensitivity to new physics and to improve its measurement accuracy. For instance, for many processes, beam polarization is a simple way to increase the signal cross section while suppressing the background. Moreover, beam polarization allows new properties to be measure (e.g., the polarization dependence of cross sections). Detailed Monte Carlo studies have shown that the ILC would be able to measure most of the standard model parameters to within sub-percent levels[10].

Because of the improved experimental accuracy intended of the ILC, theoretical predictions must be given with new level of precision. In particular, a radiative correction due to the electroweak interaction (including spin polarizations) is mandatory for such requirements. Before the discovery of the top quark, a full electroweak radiative correction was conducted for an $e^-e^+ \rightarrow t\bar{t}$ process at a lower energy[11], and was then obtained independently for higher energies[12, 13]. The same correction including radiative photon, $e^-e^+ \rightarrow t\bar{t}\gamma$ process, has also been reported[14]. However, none of previous calculations include the effect of spin polarization. In the present study, we report full electroweak radiative corrections for the process $e^-e^+ \rightarrow t\bar{t} \rightarrow b\bar{b}\mu^+\mu^-\nu_\mu\bar{\nu}_\mu$ using a narrow-width approximation for the top quarks. Spin-polarization effects are included, not only in the initial beams but also in the full spin correlations of the production and decay of top quarks.

This report is organized as follows. The calculation method is explained in Section 2. We use the GRACE-Loop system to calculate cross sections. A system-checking method is also explained in Section 2. In Section 3, we show results of electroweak corrections of the total cross section as well as the angular distribution with spin-polarized beams. The effects of radiative corrections on top-quark decay products, including a spin correlation, are also discussed using a narrow-width approximation. The contribution of an NLO-QCD correction is briefly discussed in Section 3. We summarize and conclude this report in Section 4. In Appendix A, we summarize the formulae of the NLO-QCD correction for massive quark production.

2. Calculation Method

For precise cross-section calculations of the target process in this study, we used the GRACE-Loop system, which is an automatic system for calculating cross sections of scattering processes at one-loop level for the standard theory[15] and the minimal supersymmetric standard model[16]. This system has been used to treat electroweak processes with two, three, or four particles in the final state[17, 18, 19, 20]. The GRACE-Loop system has the following features. Firstly, the renormalization of the electroweak interaction is carried out using an on-shell scheme[21, 22]. Secondly, the infrared divergences are regulated using a fictitious photon mass λ [22]. Thiedly, the symbolic manipulation

system FORM[23] is used to handle all Dirac and tensor algebras in n space time dimensions. Fourthly, GRACE generates FORTRAN source code that calls library subroutines to calculate the scattering amplitudes. Fifthly, for loop integrations, all tensor one-loop integrals are reduced to scalar integrals using our own formalism, whereupon the integrations are performed using packages FF[24] and LoopTools[25]. Finally, phase-space integrations are done using an adaptive Monte Carlo integration package BASES[26, 27]. For numerical calculations, we use quartic precision for floating-point variables.

To treat spin polarization in loop calculations, we apply the projection operators on fermion wave functions. A spin projection of the initial beams is realized simply by multiplying the spin-projection operator $P_\lambda = \frac{1}{2}(1 + \lambda\gamma_5\not{p}/m)$, where p is the four-momentum of beam particles and $\lambda = \pm 1$ is their helicity. Here, we assume that initial beams comprise light fermions with no transverse momenta. The electron/positron completeness relation becomes $\sum_s u(p)^s \bar{u}^s(p) = \frac{1}{2}(1 + \lambda\gamma_5\not{p})(\not{p} + m)$. For top quarks, the spin polarization vector can be taken as

$$s_t^\mu = \left(\frac{\mathbf{p}_t \cdot \hat{\mathbf{s}}_t}{m_t}, \hat{\mathbf{s}}_t + \frac{(\mathbf{p}_t \cdot \hat{\mathbf{s}}_t)\mathbf{p}_t}{m_t(E_t + m_t)} \right),$$

where m_t is the top-quark mass, E_t is the top-quark energy, and \mathbf{p}_t is the top-quark three-momentum. The spin is projected in the direction of the top-quark momentum direction using a direction vector $\hat{\mathbf{s}}_t = \mathbf{p}_t/|\mathbf{p}_t|$. The completeness relations in this case are given as $\sum_\lambda u(p, \lambda)\bar{u}(p, \lambda) = \frac{1}{2}(1 + \lambda\gamma_5\not{\mathbf{p}})(\not{p} + m)$ for top quarks and $\sum_\lambda v(p, \lambda)\bar{v}(p, \lambda) = \frac{1}{2}(1 + \lambda\gamma_5\not{\mathbf{p}})(\not{p} - m)$ for anti-top quarks.

In GRACE, while using the R_ξ -gauge in the linear gauge-fixing terms, the non linear gauge-fixing Lagrangian[28, 15] is employed, namely

$$\begin{aligned} \mathcal{L}_{GF} = & -\frac{1}{\xi_W} \left| \left(\partial_\mu - ie\tilde{\alpha}A_\mu - igc_W\tilde{\beta}Z_\mu \right) W^{\mu+} + \xi_W \frac{g}{2} \left(v + \tilde{\delta}H + i\tilde{\kappa}\chi_3 \right) \chi^+ \right|^2 \\ & - \frac{1}{2\xi_Z} \left(\partial \cdot Z + \xi_Z \frac{g}{2c_W} (v + \tilde{\epsilon}H) \chi_3 \right)^2 - \frac{1}{2\xi_A} (\partial \cdot A)^2, \end{aligned}$$

for the sake of system checking. Here A, Z, W, χ , and H denote the wave functions of the corresponding fields, and ξ 's are gauge parameters for the linear gauge-fixing terms. The results must be independent of the non linear gauge parameters $\{\tilde{\alpha}, \tilde{\beta}, \tilde{\delta}, \tilde{\kappa}, \tilde{\epsilon}\}$. We can perform system checking to confirm the correctness of the system. Before calculating cross sections, we checked for ultra-violet coefficient (C_{UV}) independence, photon-mass (λ) independence, and gauge invariance numerically at several randomly-chosen phase points. for instance, in the polarized case at a CM energy of 500 GeV, we confirmed

	$(C_{UV}, \lambda, \tilde{\alpha}, \tilde{\beta}, \tilde{\delta}, \tilde{\kappa}, \tilde{\epsilon})$ (0, 10^{-17} , 0, 0, 0, 0, 0)	$(C_{UV}, \lambda, \tilde{\alpha}, \tilde{\beta}, \tilde{\delta}, \tilde{\kappa}, \tilde{\epsilon})$ (0, 10^{-17} , 10, 20, 30, 40, 50)
$e_L^- e_R^+$	-0.247141016563629897981294517	-0.247141016563629897981294591
$e_R^- e_L^+$	-0.103981906801174833889546868	-0.103981906801174833889546851

Table 1: Non linear gauge-parameter independence of amplitude. The results are stable over 25 digits using quartic-precision variables.

ultra-violet coefficient and photon-mass independence, both with stable results over 19 digits, when parameters C_{UV} and λ changed by three orders of magnitude from their nominal values. Meanwhile, the non linear gauge-invariance results are stable over 25 digits against changing those values, as shown in Table 1. We note that the parameter dependence of the amplitude is logarithmic for C_{UV} and λ , whereas it is up to quartic for the non linear gauge parameters.

In addition to the above checks, we examined the soft-photon cut-off independence: for cross sections at the one-loop level, the results must be independent of a hard-photon cut-off parameter k_c . We confirmed that the integration results are self-consistent within the statistical error of numerical phase-space integrations while varying k_c from 10^{-4} GeV to 10^{-1} GeV.

3. Results and discussions

For cross-section calculations of the production process $e^-e^+ \rightarrow t\bar{t}$ and its sequential top decay, we use the input parameters listed in Table 2. The masses of the light quarks (i.e., other than the top quark) and W boson are chosen to be consistent with low-energy experiments[29]. Other particle masses are taken from recent measurements[3]. The weak mixing angle is obtained using the on-shell condition $\sin^2 \theta_W = 1 - m_W^2/m_Z^2$ because of our renormalization scheme. The fine-structure constant $\alpha = 1/137.0359859$ is taken from the low-energy limit of Thomson scattering, again because of our renormalization scheme. The W -boson width is taken as a calculated value at tree level using the same parameters as above.

3.1. Production Cross Sections

We focus on CM energies from 500-1000 GeV to avoid possible complications from large QCD corrections near the production threshold. In the energy region, a target of top-quark physics is a precise measurement of the Z -top and top-Yukawa couplings. It is reasonable to expect that information beyond the standard theory could be probed through precise measurements of a top-production form factor[30]. To extract new physics from the form-factor measurement, one has to understand precisely the effects of higher-order corrections on the measurements.

For the $e^-e^+ \rightarrow t\bar{t}$ process, there are four Feynman diagrams at tree level, 16 with real-photon radiation, and 150 at the one-loop level. Typical diagrams are shown in Fig 1. We calculate the total cross sections as a function of CM energy of 500-1000 GeV assuming 100% left-hand polarization for electrons (e_L^-) and 100% right hand polarization positrons (e_R^+), or vice versa (e_R^- and e_L^+). We omit cross sections involving $e_L^-e_L^+$

u -quark mass	58.0×10^{-3} GeV	d -quark mass	58.0×10^{-3} GeV
c -quark mass	1.5 GeV	s -quark mass	92.0×10^{-3} GeV
t -quark mass	173.5 GeV	b -quark mass	4.7 GeV
Z -boson mass	91.187 GeV	W -boson mass	80.370 GeV
Higgs mass	126 GeV	W -boson width	1.993 GeV

Table 2: Input parameters

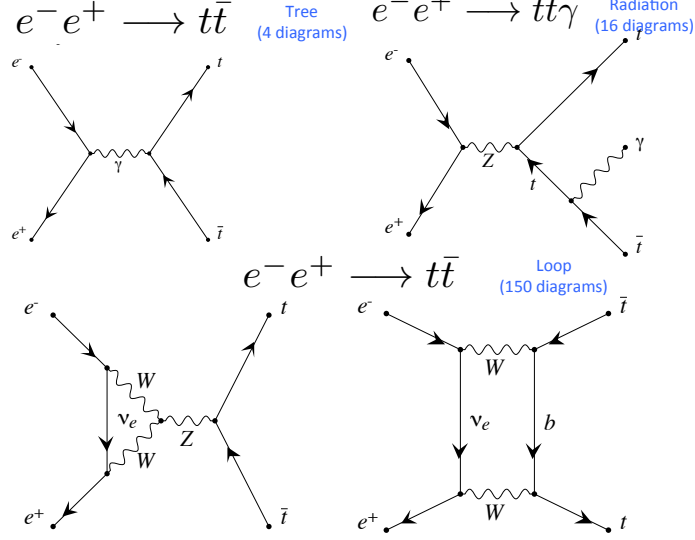


Figure 1: Examples of Feynman diagrams for $e^-e^+ \rightarrow t\bar{t}$ at tree level, with real radiation and at loop level.

and $e_R^-e_R^+$ collisions because they yield negligible contributions. The cross sections so obtained are shown in Fig. 2 as functions of the colliding energy. As shown in the upper panels of Fig. 2, the total cross sections for the $e_L^-e_R^+$ collision are roughly twice those for the $e_R^-e_L^+$ collision due to the P -violation of the weak interaction. When design values of polarizations ($e_L^- = 80\%$ and $e_R^+ = 30\%$) can be realized at the ILC, we will gain roughly 50% in total cross section compared with the non-polarized case. In addition, the total amount of electroweak corrections is smaller for the $e_R^-e_L^+$ case than that for the $e_L^-e_R^+$ case. For a simple evaluation of the fraction of higher-order corrections, let us introduce a ratio $\delta = (\sigma_{NLO} - \sigma_{Tree})/\sigma_{Tree}$, where σ_{NLO} and σ_{Tree} are the total cross sections at a full $\mathcal{O}(\alpha)$ correction and that at tree level, respectively. The results so obtained are summarized in Fig. 3. For instance, at a CM energy of 500 GeV, the electroweak correction of $e_L^-e_R^+$ is -0.8% and the electroweak correction of $e_R^-e_L^+$ is 12% . At a CM energy of 1000 GeV, the electroweak correction of $e_L^-e_R^+$ is 4.0% , whereas the electroweak correction of $e_R^-e_L^+$ is 26% . The $e_R^-e_L^+$ polarization has larger radiative corrections than does the $e_L^-e_R^+$ one. Together with the larger cross sections, one can expect smaller systematic errors for the cross-section measurement with the polarized beam than in the non-polarized case. We note that the full electroweak correction reported here includes a trivial photonic correction from the initial-state photon radiation (ISR). It is known that the ISR correction can be factorized and be improved using higher-order re-summation[22]. Although further improvements of precise predictions of cross sections are possible by means of the parton shower method, we do not use that in this study. The polarization asymmetry of electroweak corrections may be induced by diagrams involving W bosons[31], i.e., the diagrams shown in Fig. 1. In this report, we do not discuss the origin of the radiative-correction asymmetry in detail.

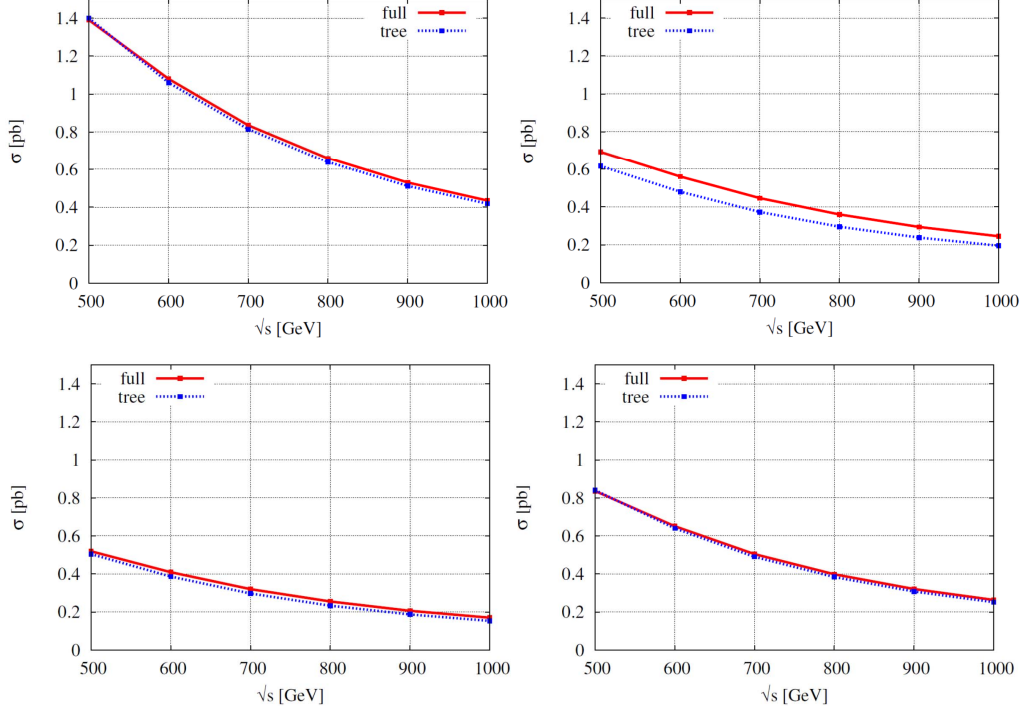


Figure 2: Total cross sections with respect to the CM energy \sqrt{s} from 500 GeV to 1000 GeV, assuming 100% of e_L^- and e_R^+ for the upper-left figure, and vice versa (e_R^- and e_L^+) for the upper-right figure. Lower-left and lower-right figures show cross sections with non-polarization and polarization with a design value ($e_L^- = 80\%$ and $e_R^+ = 30\%$, respectively). The dotted lines show the results for the tree level while the solid lines correspond to the full one-loop electroweak correction.

3.2. Angular distributions

The angular distribution of the top-pair production has a large forward peak, thus it has a sizable forward-backward asymmetry that allows us to make a good test of the standard theory. However, radiative corrections may distort the angular distribution as well as the total cross sections. Angular distributions of the top-pair production with and without radiative corrections at the CM energy of 500 GeV are shown in Fig. 4 for both $e_L^-e_R^+$ (left figure) and $e_R^-e_L^+$ (right figure) polarizations. The ISR corrections generally flatten the forward peak because of a smearing effect of the CM system. One can see this smearing effect clearly in the $e_L^-e_R^+$ polarization case. Even though the total correction δ is small at $\sqrt{s} = 500$ GeV as mentioned above, the electroweak correction modifies the angular distribution. A small correction to the total cross section is caused by an accidental cancellation between negative corrections for the forward region and a positive contribution in the backward region. In contrast, the electroweak correction for the $e_R^-e_L^+$ polarization gives positive corrections in the whole angular region, as shown in the right-hand panel in Fig. 4. In conclusion, the observed value of the forward-backward asymmetry is largely affected by the electroweak radiative corrections. Moreover, the

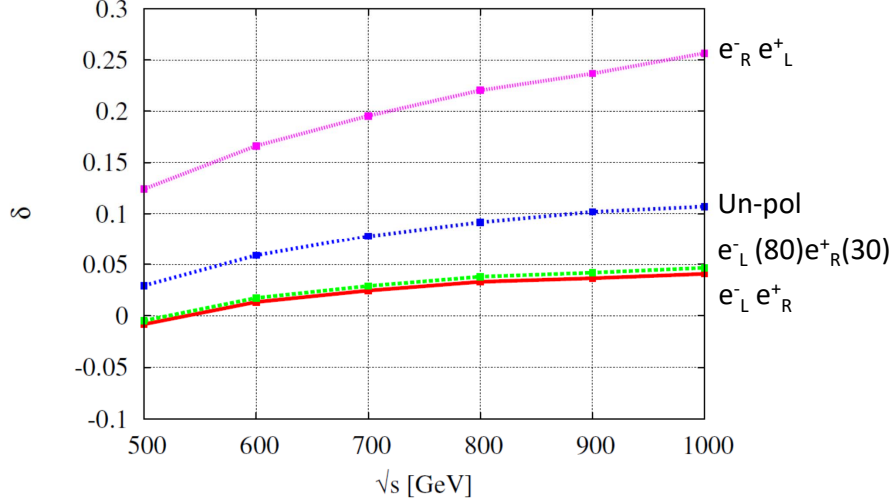


Figure 3: Ratio of the full correction δ for various polarization conditions. From the top of the figure, the lines show $e^-_R e^+_L$ polarization, non-polarization, design polarization, and $e^-_L e^+_R$ polarization, in that order.

effect of the radiative corrections depends on the spin-polarization of the initial beams. Therefore, careful investigations of the forward-backward asymmetry are required.

A definition of the forward-backward asymmetry is given as follows. The forward and back-ward cross sections are defined as $\sigma_F = \int_0^1 d\sigma/d\cos\theta_t d\cos\theta_t$ and $\sigma_B = \int_{-1}^0 d\sigma/d\cos\theta_t d\cos\theta_t$, respectively. Thus, the forward-backward asymmetry is defined by $A_{FB} = (\sigma_F - \sigma_B)/(\sigma_F + \sigma_B)$. The tree and electroweak corrected values of the forward-backward asymmetry are summarized in Table 3. For $e^-_L e^+_R$ ($e^-_R e^+_L$) polarization, the forward-backward asymmetry at tree level is 0.385 (0.467), which becomes 0.317 (0.443) after the full electroweak correction. When the design values of polarizations are assumed, the forward-backward asymmetry is determined mainly by the contribution from the $e^-_L e^+_R$ component, as shown in the last row of Table 3.

3.3. Top-quark decay

According to the beam polarization, the produced top quarks are also polarized. The polarization degree is defined as $\delta_{pol} = (\sigma_L - \sigma_R)/(\sigma_L + \sigma_R)$, where σ_L and σ_R are the

$e^-e^+ \rightarrow t\bar{t}$	$A_{FB}(\text{Tree})$	$A_{FB}(\text{Full})$
e^-e^+	0.410	0.359
$e^-_L e^+_R$	0.385	0.317
$e^-_R e^+_L$	0.467	0.443
$e^-_L(80\%)e^+_R(30\%)$	0.388	0.321

Table 3: Estimated values of the forward-backward asymmetry

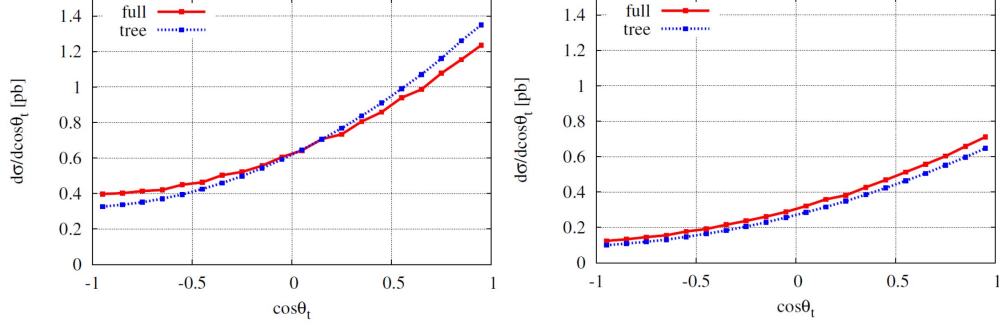


Figure 4: Angular distributions of the production angle of top quark θ_{top} at a CM energy of 500 GeV with $e_L^- e_R^+$ polarization (left) and $e_R^- e_L^+$ polarization (right). The dotted lines show tree-level results whereas the solid lines show full electroweak-corrected results.

cross sections for creating left-handed and right-handed top quarks, respectively. The polarization degree depends on the CM energy, as shown in Fig. 5. At tree level, the polarization degree increases from 8.8% at 350 GeV to 67.6% at 800 GeV. At a CM energy of 350 GeV (close to the production threshold), the produced top quark moves slowly and thus its helicity state is easily flipped. In contrast, at higher energies, the particle moves much faster and the helicity is stable. That causes the difference in polarization to increase with energy, as shown in Fig. 5. The full electroweak corrections reduce the polarization degree by roughly 10% in the high-energy region. The top quark immediately decays into a bottom (b) quark and a fermion pair. Because the angular and energy distributions of the decay products depend strongly on the top polarization, an exact treatment of the top polarization is necessary. We discuss the top decay of $t \rightarrow b\mu^+\nu_\mu$ at a CM energy of 500 GeV as a benchmark process. Because b-quark tagging is required to identify the top quark experimentally, precise calculation of b-quark distributions is important.

The number of Feynman diagrams for the six-body final-state $e^- e^+ \rightarrow b\bar{b}\mu^-\mu^+\nu\bar{\nu}$ is too large, thus a full electroweak correction is impossible using the current computing power. Instead, we have used a “narrow width approximation” for the top-quark production and decay, including the spin correlation exactly. The branching ratio of the $b\mu^+\nu_\mu$ decay is obtained with the $\mathcal{O}(\alpha)$ correction as follows: the top width at tree level is calculated to be $\Gamma^{Tree} = 1.38$ GeV. The full electroweak-corrected width is calculated by summing all possible decay channels of $t \rightarrow b\ell\nu_\ell$ and $t \rightarrow bq\bar{q}$ as $\Gamma^{Loop} = 1.77$ GeV. The partial width of the decay channel to $b\mu^+\nu_\mu$ is 0.188 GeV, thus the branching ratio of this channel is obtained as 10.6% after the $\mathcal{O}(\alpha)$ correction.

The total cross section of N -body production including a narrow fermion-resonance with mass m and width Γ , which decays into N bodies, can be expressed as

$$\begin{aligned}\sigma &= \frac{1}{flux} \int |\mathcal{M}|^2 d\Omega_N \\ &= \frac{1}{flux} \int \frac{|\sum_\lambda \mathcal{M}_p u_\lambda(q) \bar{u}_\lambda(q) \mathcal{M}_d|^2}{(q^2 - m^2)^2 + m^2 \Gamma^2} \frac{dq^2}{2\pi} d\cos\theta_q d\varphi_q d\Omega_n d\Omega_{N-n},\end{aligned}$$

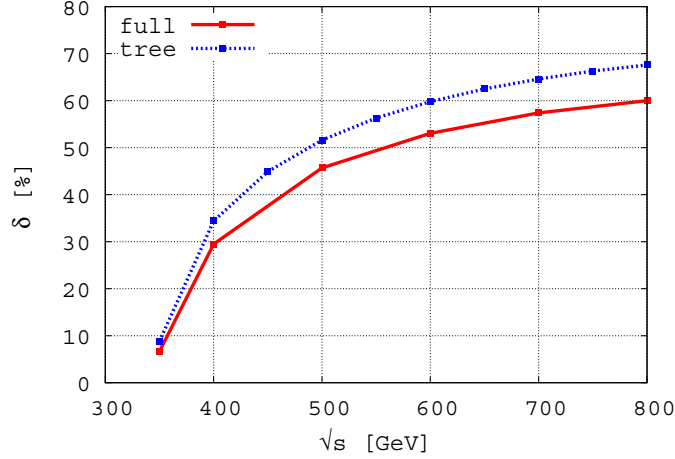


Figure 5: Top-quark polarization as a function of CM energy from 300 GeV to 800 GeV for the process $e_L^- e_R^+ \rightarrow t\bar{t}$.

where u_λ is the spinor, q_μ is the momentum (off-shell), and λ is the spin of the resonance particle. The term $d\Omega_n$ denotes an n -body phase space, and \mathcal{M}_p and \mathcal{M}_d are the product and decay amplitudes, respectively. Using an on-shell approximation as $q^2 \sim q_0^2 = m^2$ for the numerator, the amplitudes can be approximated as $\tilde{\mathcal{M}}_p^\lambda = \mathcal{M}_p u_\lambda(q_0)$ and $\tilde{\mathcal{M}}_d^\lambda = \mathcal{M}_d u_\lambda(q_0)$. Therefore, the total cross section becomes

$$\sigma \simeq \frac{1}{flux} \sum_\lambda \int |\tilde{\mathcal{M}}_p^\lambda|^2 d\cos\theta_q d\varphi_q d\Omega_{N-n} \int |\tilde{\mathcal{M}}_d^\lambda|^2 d\Omega_n \int \frac{1}{(q^2 - m^2)^2 + m^2 \Gamma^2} \frac{dq^2}{2\pi}.$$

We note that the spin correlation is maintained between production and decay. Integration can be performed over the resonance masses, namely

$$\int |\tilde{\mathcal{M}}_d^\lambda|^2 d\Omega_n \int_{-\infty}^{+\infty} \frac{1}{(q^2 - m^2)^2 + m^2 \Gamma^2} \frac{dq^2}{2\pi} = \frac{1}{\Gamma} \frac{1}{2m} \int |\tilde{\mathcal{M}}_d^\lambda|^2 d\Omega_n,$$

which gives the branching ratio of a specific decay channel. In reality, calculations are performed using the exact six-body phase space. The validity of the narrow-width approximation is verified by comparing b-quark distributions obtained by the narrow-width approximation and the exact six-body calculations at tree level.

the angular and energy-distributions of b quarks are shown in Fig. 6 and 7, respectively. For the $e_L^- e_R^+$ polarization case, the decayed b quarks tend to be produced in the forward direction of the top-quark momentum, and in the forward direction for the $e_R^- e_L^+$ polarization. The angular distributions of the b quarks at tree-level reflect this tendency. The electroweak corrections distort the angular distribution rather largely in the $e_L^- e_R^+$

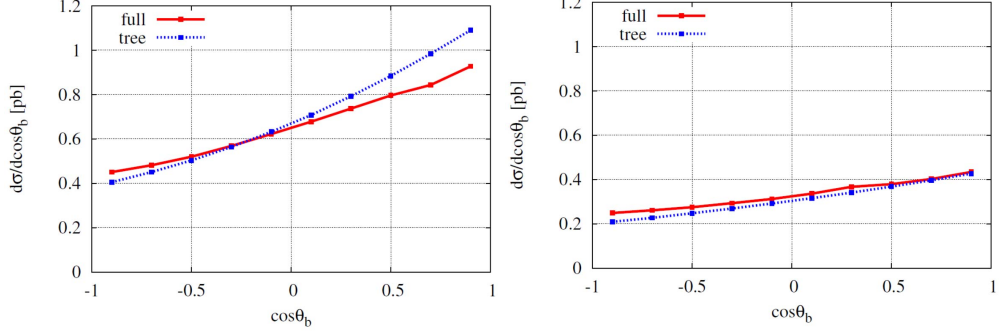


Figure 6: Angular distributions of b quarks with $e_L^- e_R^+$ (left) and $e_R^- e_L^+$ (right) polarizations. Dotted lines and solid lines show tree and electroweak corrected distributions, respectively.

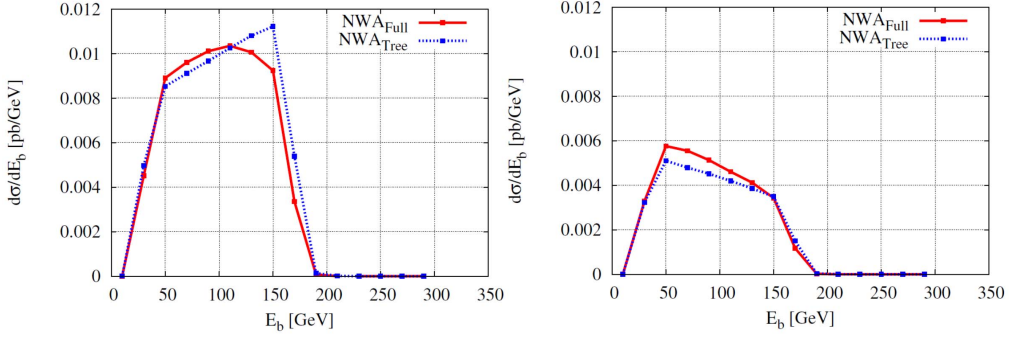


Figure 7: Energy distributions of b quarks with $e_L^- e_R^+$ (left) and $e_R^- e_L^+$ (right) polarizations. Dotted lines and solid lines show tree and electroweak corrected distributions, respectively.

polarization case, as shown in the left-hand panel of Fig. 6. In the top-quark rest frame, the b-quark energy is monochromatic (while ignoring the W -boson width). Thus, the energy distribution of the b quarks are a reflection of their angular distribution with respect to the top-quark momentum, after the Lorentz boost due to finite top-momentum. From this point on view, the energy distribution of b-quarks can be understood intuitively. Again, the electroweak corrections distort the distribution largely for the $e_L^- e_R^+$ case, as shown in Fig. 7.

3.4. QCD correction

We have not discussed the QCD correction so far in this report because the QCD correction for the top-pair production is independent of the beam polarization and simply modifies the total cross section while maintaining the distributions. However, the QCD correction is not small at a CM energy of 500 GeV. The formulae used here are summarized in Appendix A. While the QCD correction is expected to be $\alpha_s/\pi \simeq 3.8\%$

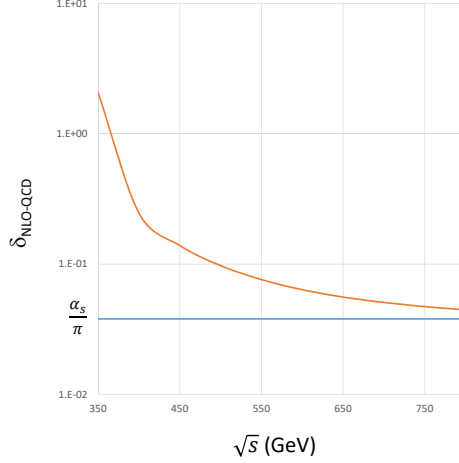


Figure 8: NLO-QCD correction of the top-pair production process. A strong coupling constant $\alpha_s = 0.12$ is used.

at higher energies it still makes a contribution of 9.7% to the total cross section at a CM energy of 500 GeV. While the QCD correction gradually approaches the asymptotic value of α_s/π with increase of the CM energy, as shown in Fig. 8, it still makes a large contribution around a CM energy of 500 GeV. For future experimental analysis, the QCD corrections around these energies must be investigated more precisely.

4. Summary and Conclusions

In this report, we have present full $\mathcal{O}(\alpha)$ electroweak corrections for the $e^-e^+ \rightarrow t\bar{t}$ process associated with the sequential decay $t \rightarrow b\mu\nu_\mu$. Calculations were performed using the GRACE-Loop system. The electroweak radiative correction was estimated typically as a level of 10% on the total cross section in the on-shell scheme for the non-polarized case. Wheres the cross section with $e_L^-e_R^+$ polarization was roughly twice that with $e_R^-e_L^+$ polarization at tree level, the radiative correction of the former was smaller than that of the latter. The electroweak correction with the design polarizations ($e_L^- = 80\%$ and $e_R^+ = 30\%$) was estimated to be less than 5%. Even though the electroweak correction of the total cross sections was rather small for $e_L^-e_R^+$ polarization, the radiative corrections modified the angular distribution of the produced top quarks. The radiative corrections decreased the forward-backward asymmetry of the top-quark production from 0.388 to 0.321 for the design polarization. We also studied the properties of

top-quark decay $t \rightarrow b\mu^+\nu_\mu$ including the spin correlation. Both production and decay processes were calculated with $\mathcal{O}(\alpha)$ corrections and combined with using the narrow-width approximation. We observed the energy distribution of b-quarks to be largely distorted because of the radiative correction. Therefore, an event generator including radiative corrections for both production and decay with the spin correlation will be necessary for precise measurements in future ILC experiments. Because the NLO-QCD correction is still large at CM energies 500 GeV, a precise QCD correction is also desired.

The authors wish to thank Prof. J. Vermaseren for his continuous encouragement and fruitful discussions. T.U. is supported by the ERC Advanced Grant No.320651 ‘‘HEPGAME’’.

Appendix A. QCD correction

The detailed formulae of the NLO-QCD correction for massive quark-pair production by electroweak interaction are summarized in this Appendix. In following calculations, the standard $\overline{\text{MS}}$ renormalization scheme is used. After renormalization, a space-time dimension other than four is reinterpreted to regulate the infrared divergence as $d = 4 - 2\varepsilon_{UV} \rightarrow 4 + 2\varepsilon_{IR}$ with $\varepsilon_{IR} > 0$. The NLO-QCD correction consists of three parts: vertex, self-energy, and real-gluon-emission corrections. The contributions of each part is given separately below.

Vertex correction

The total vertex correction is given as

$$\Gamma = C_F (I_k + I_0),$$

where $C_F = 4/3$ is a color factor. Each integration term is given as

$$\begin{aligned} I_k &= \frac{\alpha_s}{4\pi} \left\{ \frac{-1}{\varepsilon_{IR}} + \left(L' + \log \mu_t + 1 + \tilde{\mu}_t \log \left(-\frac{1 - \tilde{\mu}_t}{1 + \tilde{\mu}_t} \right) \right) \right\}, \\ I_0 &= \frac{\alpha_s}{4\pi} \left\{ \frac{1}{\varepsilon_{IR}} \frac{2(2\mu_t + 1)}{\tilde{\mu}_t} \log \left(-\frac{1 - \tilde{\mu}_t}{1 + \tilde{\mu}_t} \right) - 1 - \frac{2(2\mu_t + 1)}{\tilde{\mu}_t} \left(Sp \left(\frac{1}{2} - \frac{1}{2\tilde{\mu}_t} \right) - Sp \left(\frac{1}{2} + \frac{1}{2\tilde{\mu}_t} \right) \right) \right. \\ &\quad + \frac{2}{\tilde{\mu}_t} \log \left(-\frac{1 - \tilde{\mu}_t}{1 + \tilde{\mu}_t} \right) (-2(6\mu_t + 1)) \\ &\quad \left. + (2\mu_t + 1) \left[L' + \frac{1}{2} \log \left(-\frac{1 - \tilde{\mu}_t}{1 + \tilde{\mu}_t} \right) + \log \left(-\frac{\tilde{\mu}_t(\tilde{\mu}_t + 1)}{2} \right) \right] \right\}, \\ L' &= \log \left(\frac{-s}{\mu_F} \right), \quad \mu_t = -\frac{m_t^2}{s}, \quad \tilde{\mu}_t = \sqrt{4\mu_t + 1}, \end{aligned}$$

where μ_F is the factorization energy scale, m_t is the top-quark mass, and s is the momentum square of a $t\bar{t}$ -system.

Self-energy correction

The self-energy correction appears because of the renormalization scheme. The top mass that appears here must be interpreted as the $\overline{\text{MS}}$ mass:

$$\Sigma(p^2 = m_t^2) = C_F \frac{\alpha_s}{4\pi} \left\{ \frac{-1}{\varepsilon_{IR}} + (L_t - 4) \right\},$$

where $L_t = \log(m_t^2/\mu_F^2)$.

Real-emission correction

The real-emission correction is further separated into two parts: soft-gluon emission and hard-gluon emission. A threshold energy k_c is introduced to separate soft and hard emissions. The soft-emission corrections are given as

$$\begin{aligned} R_{ii} &= C_F \frac{\alpha_s}{2\pi} \left\{ \frac{1}{\varepsilon_{IR}} - L_k - \frac{1}{\tilde{\mu}_t} \log \left(-\frac{1 - \tilde{\mu}_t}{1 + \tilde{\mu}_t} \right) \right\}, \\ R_{ij} &= C_F \frac{\alpha_s}{2\pi} \left\{ \frac{-1}{\varepsilon_{IR}} \left(\frac{2\mu_t + 1}{\tilde{\mu}_t} \right) \log \left(-\frac{1 - \tilde{\mu}_t}{1 + \tilde{\mu}_t} \right) \right. \\ &\quad \left. - \frac{2\mu_t + 1}{\tilde{\mu}_t} \left(L_k \log \left(-\frac{1 - \tilde{\mu}_t}{1 + \tilde{\mu}_t} \right) + Sp \left(\frac{2}{1 + 1/\tilde{\mu}_t} \right) - Sp \left(\frac{2}{1 - 1/\tilde{\mu}_t} \right) \right) \right\}, \end{aligned}$$

where $L_k = 2 \log(2k_c/\mu_F)$. These formulae are obtained via an approximation in which the gluon energy is much smaller than m_t . The hard-emission cross section can be calculated using the GRACE system based on the exact matrix element. We confirmed numerically that real-emission corrections are independent of k_c , whose values are below 1 GeV.

Total correction

The NLO-QCD cross section σ_{NLO} can be obtained as

$$\sigma_{NLO} = \left\{ 1 + 2(R_{ii} + R_{ij} + \text{Re}[\Gamma + \Sigma]) \right\} \sigma_0 + \sigma_g,$$

where σ_0 and σ_g are the Born and hard-emission cross sections, respectively. After summing up all contributions, the infrared divergence and μ_F dependence disappear completely.

References

- [1] G. Aad, et al., Observation of a new particle in the search for the Standard Model Higgs boson with the ATLAS detector at the LHC, Phys. Lett. B716 (2012) 1–29. doi:10.1016/j.physletb.2012.08.020.
- [2] S. Chatrchyan, et al., Observation of a new boson at a mass of 125 GeV with the CMS experiment at the LHC, Phys. Lett. B716 (2012) 30–61. doi:10.1016/j.physletb.2012.08.021.
- [3] C. Patrignani, et al., Review of Particle Physics, Chin. Phys. C40 (10) (2016) 100001. doi:10.1088/1674-1137/40/10/100001.
- [4] [link].
URL <https://twiki.cern.ch/twiki/bin/view/AtlasPublic/SupersymmetryPublicResults>

- [5] [link].
URL <https://twiki.cern.ch/twiki/bin/view/CMSPublic/PhysicsResultsSUS>
- [6] S. Alekhin, A. Djouadi, S. Moch, The top quark and higgs boson masses and the stability of the electroweak vacuum, *Physics Letters B* 716 (1) (2012) 214 – 219. doi:<http://dx.doi.org/10.1016/j.physletb.2012.08.024>.
URL [//www.sciencedirect.com/science/article/pii/S0370269312008611](http://www.sciencedirect.com/science/article/pii/S0370269312008611)
- [7] T. Behnke, J. E. Brau, B. Foster, J. Fuster, M. Harrison, J. M. Paterson, M. Peskin, M. Stanitzki, N. Walker, H. Yamamoto, The International Linear Collider Technical Design Report - Volume 1: Executive Summary [arXiv:1306.6327](https://arxiv.org/abs/1306.6327).
- [8] C. Adolphsen, M. Barone, B. Barish, K. Buesser, P. Burrows, J. Carwardine, J. Clark, H. Mainaud Durand, G. Dugan, E. Elsen, et al., The International Linear Collider Technical Design Report - Volume 3.I: Accelerator & in the Technical Design Phase [arXiv:1306.6353](https://arxiv.org/abs/1306.6353).
- [9] C. Adolphsen, M. Barone, B. Barish, K. Buesser, P. Burrows, J. Carwardine, J. Clark, H. Mainaud Durand, G. Dugan, E. Elsen, et al., The International Linear Collider Technical Design Report - Volume 3.II: Accelerator Baseline Design [arXiv:1306.6328](https://arxiv.org/abs/1306.6328).
- [10] H. Baer, T. Barklow, K. Fujii, Y. Gao, A. Hoang, S. Kanemura, J. List, H. E. Logan, A. Nomerotski, M. Perelstein, et al., The International Linear Collider Technical Design Report - Volume 2: Physics [arXiv:1306.6352](https://arxiv.org/abs/1306.6352).
- [11] J. Fujimoto, Y. Shimizu, Radiative Corrections to $e^+e^- \rightarrow t\bar{t}$ in Electroweak Theory, *Mod. Phys. Lett. A* (1988) 581. doi:[10.1142/S0217732388000696](https://doi.org/10.1142/S0217732388000696).
- [12] J. Fleischer, T. Hahn, W. Hollik, T. Riemann, C. Schappacher, A. Werthenbach, Complete electroweak one loop radiative corrections to top pair production at TESLA: A Comparison [arXiv:hep-ph/0202109](https://arxiv.org/abs/hep-ph/0202109).
- [13] J. Fleischer, A. Leike, T. Riemann, A. Werthenbach, Electroweak one-loop corrections for e^+e^- -annihilation into $t\bar{t}$ including hard bremsstrahlung, *The European Physical Journal C - Particles and Fields* 31 (1) (2003) 37–56. doi:[10.1140/epjc/s2003-01263-8](https://doi.org/10.1140/epjc/s2003-01263-8).
- [14] P. H. Khem, J. Fujimoto, T. Ishikawa, T. Kaneko, K. Kato, Y. Kurihara, Y. Shimizu, T. Ueda, J. A. M. Vermaseren, Y. Yasui, Full $\mathcal{O}(\alpha)$ electroweak radiative corrections to $e^+e^- \rightarrow t\bar{t}\gamma$ with grace-loop, *The European Physical Journal C* 73 (4) (2013) 2400. doi:[10.1140/epjc/s10052-013-2400-3](https://doi.org/10.1140/epjc/s10052-013-2400-3).
- [15] G. Bélanger, F. Boudjema, J. Fujimoto, T. Ishikawa, T. Kaneko, K. Kato, Y. Shimizu, Automatic calculations in high energy physics and grace at one-loop, *Physics Reports* 430 (3) (2006) 117 – 209. doi:<http://dx.doi.org/10.1016/j.physrep.2006.02.001>.
- [16] J. Fujimoto, T. Ishikawa, Y. Kurihara, M. Jimbo, T. Kon, M. Kuroda, Two-body and three-body decays of charginos in one-loop order in the mssm, *Phys. Rev. D* 75 (2007) 113002. doi:[10.1103/PhysRevD.75.113002](https://doi.org/10.1103/PhysRevD.75.113002).
- [17] G. Bélanger, F. Boudjema, J. Fujimoto, T. Ishikawa, T. Kaneko, Y. Kurihara, K. Kato, Y. Shimizu, Full $\mathcal{O}(\alpha)$ electroweak corrections to double higgs-strahlung at the linear collider, *Physics Letters B* 576 (2003) 152 – 164. doi:<http://dx.doi.org/10.1016/j.physletb.2003.09.080>.
- [18] G. Bélanger, F. Boudjema, J. Fujimoto, T. Ishikawa, T. Kaneko, K. Kato, Y. Shimizu, Y. Yasui, Full $\mathcal{O}(\alpha)$ electroweak and $\mathcal{O}(\alpha_s)$ corrections to $e^+e^- \rightarrow t\bar{t}h$, *Physics Letters B* 571 (2003) 163 – 172. doi:<http://dx.doi.org/10.1016/j.physletb.2003.07.072>.
- [19] G. Bélanger, F. Boudjema, J. Fujimoto, T. Ishikawa, T. Kaneko, K. Kato, Y. Shimizu, Full $\mathcal{O}(\alpha)$ corrections to $e^+e^- \rightarrow \nu\bar{\nu}h$ by grace, *Nuclear Physics B - Proceedings Supplements* 116 (2003) 353 – 357, proceedings of the 6th International Symposium on Radiative Corrections and the 6th Zeuthen Workshop on Elementary Particle Theory. doi:[http://dx.doi.org/10.1016/S0920-5632\(03\)80198-6](http://dx.doi.org/10.1016/S0920-5632(03)80198-6).
- [20] K. Kato, F. Boudjema, J. Fujimoto, T. Ishikawa, T. Kaneko, Y. Kurihara, Y. Shimizu, Y. Yasui, Radiative corrections for Higgs study at the ILC, *PoS HEP2005* (2006) 312.
- [21] K.-i. Aoki, Z. Hioki, R. Kawabe, M. Konuma, T. Muta, Electroweak theoryframework of on-shell renormalization and study of higher-order effects, *Progress of Theoretical Physics Supplement* 73 (1982) 1. doi:[10.1143/PTPS.73.1](https://doi.org/10.1143/PTPS.73.1).
- [22] J. Fujimoto, M. Igarashi, N. Nobuya, S. Yoshimitsu, T. Keijiro, Radiative corrections to e+e reactions in electroweak theory, *Progress of Theoretical Physics Supplement* 100 (1990) 1. doi:[10.1143/PTPS.100.1](https://doi.org/10.1143/PTPS.100.1).
- [23] J. A. M. Vermaseren, New features of FORM, For the newest verion of FORM, see [?]. [arXiv:math-ph/0010025](https://arxiv.org/abs/math-ph/0010025).
- [24] G. J. van Oldenborgh, FF: A Package to evaluate one loop Feynman diagrams, *Comput. Phys. Commun.* 66 (1991) 1–15. doi:[10.1016/0010-4655\(91\)90002-3](https://doi.org/10.1016/0010-4655(91)90002-3).
- [25] T. Hahn, M. Perez-Victoria, Automatized one loop calculations in four-dimensions and D-

- dimensions, Comput. Phys. Commun. 118 (1999) 153–165. doi:[10.1016/S0010-4655\(98\)00173-8](https://doi.org/10.1016/S0010-4655(98)00173-8).
- [26] S. Kawabata, A new monte carlo event generator for high energy physics, Computer Physics Communications 41 (1) (1986) 127 – 153. doi:[http://dx.doi.org/10.1016/0010-4655\(86\)90025-1](https://dx.doi.org/10.1016/0010-4655(86)90025-1).
 - [27] S. Kawabata, A new version of the multi-dimensional integration and event generation package bases/spring, Computer Physics Communications 88 (2) (1995) 309 – 326. doi:[http://dx.doi.org/10.1016/0010-4655\(95\)00028-E](https://dx.doi.org/10.1016/0010-4655(95)00028-E).
 - [28] F. Boudjema, E. Chopin, Double Higgs production at the linear colliders and the probing of the Higgs selfcoupling, Z. Phys. C73 (1996) 85–110. doi:[10.1007/s002880050298](https://doi.org/10.1007/s002880050298).
 - [29] P. Khiem, Y. Kurihara, J. Fujimoto, T. Ishikawa, T. Kaneko, K. Kato, N. Nakazawa, Y. Shimizu, T. Ueda, J. Vermaseren, Y. Yasui, Full electroweak radiative corrections to at the ilc with grace-loop, Physics Letters B 740 (2015) 192 – 198. doi:[http://dx.doi.org/10.1016/j.physletb.2014.11.048](https://dx.doi.org/10.1016/j.physletb.2014.11.048).
 - [30] P. H. Khiem, E. Kou, Y. Kurihara, F. Le Diberder, Probing New Physics using top quark polarization in the $e^+e^- \rightarrow t\bar{t}$ process at future Linear Colliders, 2015. arXiv:1503.04247. URL <https://inspirehep.net/record/1352820/files/arXiv:1503.04247.pdf>
 - [31] E. Kou, M. Tetiana, Study of the $e^+e^- \rightarrow t\bar{t} \rightarrow b\bar{b}l^+l^-\nu\bar{\nu}$ process, unpublished note (2016).